Volume 1 | Number 1 | Jan 2013 | Pages 1–100

Nanoscale

www.rsc.org/nanoscale

ROYAL SOCIETY OF CHEMISTRY

ROYAL SOCIETY OF CHEMISTRY

www.rsc.org/nanoscale

Free-standing electrochemical electrode based on Ni(OH)$_2$/3D graphene foam for nonenzymatic glucose detection

Beibei Zhan,[a] Changbing Liu,[a] Huaping Chen,[a] Huaxia Shi,[a] Lianhui Wang,[a] Peng Chen,[c]

Wei Huang*[a,b], Xiaochen Dong*[a,b]

[a]*Key Laboratory for Organic Electronics & Information Displays (KLOEID), Nanjing University of Posts and Telecommunications, Nanjing 210023, China.*

[b]*Jiangsu-Singapore Joint Research Center for Organic/Bio-Electronics & Information Displays and Institute of Advanced Materials (IAM), Nanjing Tech University, 30 South Puzhu Road, Nanjing 211816, China*

[c]*School of Chemical and Biomedical Engineering, Nanyang Technological University, Singapore*

E-mail: iamxcdong@njtech.edu.cn; iamwhuang@njtech.edu.cn

Abstract

Three-dimensional graphene foam (3DGF) is a superior sensing material because of its high conductivity, large specific surface area and wide electrochemical potential windows. In this work, hexagonal Ni(OH)$_2$ nanosheets are deposited on the surface of chemical vapor deposition grown 3DGF through a facial hydrothermal process without any auxiliary reagents. The morphology and structure of the composite are characterized by scanning electron microscopy (SEM), transmission electron microscope (TEM), Raman spectroscopy, and X-ray diffraction (XRD), respectively. Based on the Ni(OH)$_2$/3DGF composite, a free-standing electrochemical electrode is fabricated. Being employed as a nonenzymatic glucose detection electrochemical electrode, it exhibits a high sensitivity (~2.65 mAmM^{-1}cm^{-2}), low detection limit (0.34 μM) and excellent selectivity with linear response from 1 μM to 1.17 mM. The excellent sensing properties of Ni(OH)$_2$/3DGF electrode maybe attributed to the

synergistic effect of high electrocatalytic activity of $Ni(OH)_2$ nanosheets and high conductivity and large surface area of 3DGF.

1. Introduction

At present, the determination of glucose level in blood becomes the most vital parameter for medical diagnosis of diabetes. And additionally, glucose is also the most popular object in other various analytical chemical field, including food and environment monitoring, pharmaceutical analysis and control of bioprocess. Therefore, rapid, sensitive and selective detection of glucose is of great importance, and tremendous efforts have been devoted to develop and explore glucose sensors with fast response, high sensitivity, excellent selectivity and low cost. For this purpose, a large amount of glucose sensing approaches based on optical,[1] acoustic,[2] transdermal,[3] fluorescent,[4] electronic,[5] and electrochemical[6] technologies have been explored. However, depending on numerous merits such as high sensitivity, low cost, high time efficiency and simple operation, electrochemical sensors are always recognized as one of the most convenient and effective approaches for glucose determination. However, most glucose biosensors rely on glucose oxidase, which is able to identify glucose molecules quickly and accurately through catalyzing glucose to gluconic acid and H_2O_2. Owing to the enzymes activity can be easily affected by the temperature, pH value, humidity and even toxic chemicals, the complicated procedures of enzyme-based electrode (including adsorption, cross-linking, entrapment and electro-polymerization) may lead to a enzyme activity decrease in some certain.[7] Hence, great effort has been devoted to develop stable sensor named nonenzymatic glucose detector using metallic nanoparticles, metal oxide or alloys as electrocatalyst.[8,9] Among the common metal catalyst (Cu, CuO, MnO_2, NiO, $Ni(OH)_2$, and so on), Ni-based materials are widely used to construct nonenzymatic

biosensor.[10-12] In particular, $Ni(OH)_2$ is a promising electrode material in electrochemical applications due to its well-defined electrochemical redox activity.[13] And nanostructured $Ni(OH)_2$ also possesses high specific surface and electro-active area, biocompatibility, and excellent electronic conductivity, making it desirable for high performance biosensors. In addition, the straightforward prepare process and low-cost make it more appropriate electrocatalyst for glucose detection.

Graphene, a single-atom-thick monolayer of sp^2 carbon atoms arranged in a honeycomb lattice, possess high conductivity, large specific surface area and excellent optical properties.[14] It has been widely investigated to improve the performance of various devices, such as transparent conductor,[15] supercapacitor[16] and sensors[17]. Three-dimensional graphene foam (3DGF) synthesized by chemical vapor deposition (CVD) method under template-direction of 3D nickel foam[18] has recently attracted tremendous interests to be employed as the electrode material in electrochemical applications. It is believed that 3D architecture of graphene network without defects can effectively overcome the strong π-π interaction and intersheet contact resistance between graphene sheets and presents higher conductivity and larger specific surface area (up to~850 m^2g^{-1})[19] compared to chemical reduced graphene oxide sheets.[20] Besides, the freestanding electrode can be fabricated easily using CVD grown 3DGF owing to its mechanical strength and flexibility. And meanwhile, the 3DGF still remains the exciting compatibility, making it be immensely beneficial for modification and functionalization. The highly conductive 3DGF synthesized on the Ni foam skeleton also effectively increases the catalyst loading amount leading to the enhancement in electrocatalytic efficiency.[21] These outstanding performances of 3DGF provide good opportunities for biosensing in analytical chemistry fields.

In the present work, hexagonal $Ni(OH)_2$ nanosheets were synthesized on the surface of CVD grown 3DGF through in-suit hydrothermal process without any auxiliary reagents. Serving as a free-standing

electrochemical electrode, Ni(OH)$_2$/3DGF electrode exhibits high sensitivity, low detection limit, and excellent selectivity in nonenzymatic glucose electrochemical detection. The Ni(OH)$_2$/3DGF composite is therefore promising for the future development of nonenezymatic glucose sensors with improved electrochemical properties.

2. Experimental Section

2.1 Reagents and materials

Ethanol, hydrochloric acid and sodium dodecyl benzene sulfonate (SDBS) were purchased from Shanghai Lingfeng Chemical Reagent Co., Ltd (Shanghai, China). Nickel chloride hexahydrate (NiCl$_2$·6H$_2$O), sodium hydroxide (NaOH), sodium chloride (NaCl), urea, D-glucose, D-fructose, lactose, L-abcorbic acid (AA), and dopamine (DA) were obtained from Aladdin (America). All reagents were of analytical purity grade and directly used for experiments without any further purification.

2.2 Synthesis of Ni(OH)$_2$/3DGF

As described previously,[22] 3D graphene foam was synthesized by CVD method under Argon atmosphere with ethanol as precursor and nickel foam as sacrificial substrate. After CVD growth, the nickel substrate was etched by 3.0 M HCl at 80 □ overnight. And then the freestanding 3DGF dried at 60 □. To enhance the hydrophilic property, the 3D graphene foam was activated by immersed in 10 mg·mL^{-1} SDBS solution. Afterward, the pretreatment graphene foam was transferred into autoclave containing 0.3 M NiCl$_2$·6H$_2$O and 0.45 M NaOH and reacted 12 hours at 180 □. Then, the Ni(OH)$_2$/3DGF was washed three times by deionized water and fabricated free-standing electrochemical electrode.

2.3 Apparatus and electrochemical measurements

The morphology of $Ni(OH)_2$/3DGF composite was obtained using scanning electron microscope (SEM, Hitachi S-4800) and transmission electron microscope (TEM, JEOL JEM-2010). The structure of the samples were characterized using a WITeck CRM200 confocal microscopy Raman spectroscopy with 488 nm wavelength laser and a Bruker D8 Avance diffractometer using Cu Kα radiation at a scan rate of 20 °/min, respectively. All electrochemical measurements were carried out on a CHI 660C electrochemical analyzer (Shanghai China) using the conventional three-electrode configuration with 0.1 M NaOH solution as electrolyte, $Ni(OH)_2$/3DGF as working electrode, platinum plate and Ag/AgCl as counter electrode and reference electrode, respectively.

3. Results and discussion

3.1 Characterization

Fig. 1a shows the Raman spectra of bare 3DGF obtained at different points. It can be seen obviously that the Raman spectra present two prominent characteristic peaks at around 1560 and 2700 cm^{-1}, corresponding to G and 2D band of graphene, respectively. The absence of G band at around 1350 cm^{-1}, an indication of defects and disorderly carbon, indicates the CVD grown 3DGF has high quality, which ensures the 3DGF have high conductivity. By the intensity ratio of the 2D and G peak, it also can be confirmed that the 3DGF is composed by single-, double-, and multi-layers graphene (~2.5, ~1.04, and ~0.55, respectively).[23] Fig 1b shows the Raman spectra of $Ni(OH)_2$/3DGF composite. Except for the typical 2D and G peaks coming from graphene, two characteristic peaks from $Ni(OH)_2$ at ~531 cm^{-1} (longitudinal optical, LO) and ~1090 cm^{-1} (phonon modes, 2LO) can be identified clearly.[24] Fig 1c shows the XRD pattern of $Ni(OH)_2$/3DGF. It can be seen there presents two notable diffraction peaks coming from graphene at $2\theta = 26.4°$, and 54.542°, corresponding to the (002), and (004) reflections of graphitic carbon, respectively (JCPDS No. 41-1487). In addition, diffraction peaks of $Ni(OH)_2$ are well

indexed to the (100), (101), (102), (110) and (111) phases at 2θ = 33.064°, 38.541°, 52.100°, 59.052° and 62.726°, respectively (JCPDS No. 14-0117). The XRD spectrum illustrates the $Ni(OH)_2$ nanostructures grown on 3D graphene have high crystallinity. It is worth to note that there is no peaks from α-$Ni(OH)_2$ are observed in the XRD pattern, implying the high purity of β-$Ni(OH)_2$. The Raman and XRD spectra demonstrate the formation of $Ni(OH)_2$ nanosheets on the surface of 3DGF. The thermogravimetric analysis indicated the loading amount of $Ni(OH)_2$ in the composite is around 49% (weight ratio).

The surface morphologies of bare 3D graphene and $Ni(OH)_2$/3DGF composite are characterized by SEM, as shown in Fig. 2. The 3D graphene exhibits an interconnected , porous 3D framework with the porous diameter about 150-200 μm. Also, the three-dimensional network structure has the same topological structure with nickel surface and without obvious cracks and breaks (Fig. 2a). The magnification image (inset of Fig. 2a) indicates the CVD grown graphene has smooth surface. On the contrary, the surface of $Ni(OH)_2$/3DGF composite displays coarser and brighter (Fig. 2b and 2c). At higher magnification (Fig. 2d), it can be observed that the graphene surface is uniformly covered by hexagonal $Ni(OH)_2$ nanosheets. The diameter of the hexagonal $Ni(OH)_2$ nanosheet is about 120 nm.

To further elucidate the microstructure of the hexagonal $Ni(OH)_2$ nanosheets coated on the surface of 3D graphene foam, it was characterized by TEM. As shown in Fig. 3a and 3b, the $Ni(OH)_2$ nanosheets present good hexagonal structure with the dimension of ~120 nm, which is in good agreement with the SEM result. The high-resolution TEM image (Fig. 3c) clearly shows that the interplanar spacing of 0.148 nm is corresponding to the (111) plane of $Ni(OH)_2$. In addition, the inset of Fig. 3c displays selected area electron diffraction (SAED) patterns of $Ni(OH)_2$. Several well-defined ring corresponding to the diffraction planes of XRD spectrum can be observed, suggesting a good polycrystalline nature of

the $Ni(OH)_2$. With uniform distribution and high crystalline $Ni(OH)_2$ at the nanometer scale, the

$Ni(OH)_2/3DGF$ offers abundant catalytic sites for glucose.

3.2 Electrochemical behavior of Ni(OH)₂/3DGF electrode

To compare the electrochemical performance of the free-standing 3D graphene based electrodes, the

cyclic voltammograms (CV) of bare 3DGF and $Ni(OH)_2/3DGF$ electrode were measured in 0.1 M

NaOH electrolyte at scan rate of 50 mV/s, respectively. As shown in Fig. 4a, a couple of sensitive

redox peaks for $Ni(OH)_2/3DGF$ electrode are observed at the potential of 0.3 and 0.5 V, respectively,

which could be attributed to the redox reaction between $Ni(OH)_2$ and $NiO(OH)$. Furthermore, the

electrochemical signal of $Ni(OH)_2/3DGF$ electrode is great larger than that of bare 3DGF electrode,

suggesting the $Ni(OH)_2/3DGF$ electrode is suitable for high sensitive electrochemical detection.

Additionally, in the presence of 1 mM glucose, the anodic peak current recorded from the

$Ni(OH)_2/3DGF$ electrode is significantly higher than that of composite electrode without glucose.

However, the behavior of the cathodic peak current is opposite. These experiment results suggest the

excellent catalytic properties of $Ni(OH)_2$ toward the oxidation of glucose.[25] Fig. 4b displays the CVs of

$Ni(OH)_2/3DGF$ electrode in 0.1 M NaOH containing different concentrations of glucose (from 0.2 to

1.6 mM) at a scan rate of 50 mV/s. Upon the successive addition of glucose, a remarkable current and

potential increase at the anodic peak is observed, while the cathodic peak currents give rise to a slight

up shift as same as in Fig. 4a. The oxidation of glucose to glucolactone at the $Ni(OH)_2/3DGF$ electrode

is electrocatalyzed by $NiO(OH)/Ni(OH)_2$ redox couple according to the following reactions:[26]

$$Ni(OH)_2 + OH^- \rightarrow NiO(OH) + H_2O + e^- \qquad (1)$$

$$NiO(OH) + glucose \rightarrow Ni(OH)_2 + glucolactone \qquad (2)$$
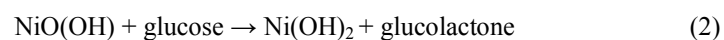
The increase of anodic peak current is contributed to excellent electrocatalytic activity of $Ni(OH)_2$ on

glucose oxidation, which is accompanied with the oxidation of Ni^{2+} to Ni^{3+}, like equation (1). Besides, due to the absorption of glucose and the oxidized intermediates on the active sites of Ni-based electrode, the anodic peak potential shifts to a positive direction.[27] As for another reason, it is attributed to the diffusion limitation of glucose at the electrode surface.[28] These results are consistent with the previous literatures.[29,30] On the other hand, there is no doubt that the oxidation of glucose consumes a few of Ni^{3+}, which cuts down the cathodic peak current slightly. Fig. 4c shows the effect of scan rate on glucose oxidation at the $Ni(OH)_2$/3DGF electrode in 0.1 M NaOH containing 1mM glucose. It can be seen the anodic peak behaves a significantly positive shift and the cathodic peak moves negatively with the increase of scan rate. These phenomena indicate that the redox reaction of $Ni(OH)_2$ on graphene is rapid and reversible. Moreover, the anodic peak potential shifts positively, suggesting that there is a kinetic limitation in the reaction of glucose oxidation.[31] Furthermore, Fig. 4d demonstrates both anodic and cathodic peak currents from $Ni(OH)_2$/3DGF electrode linearly scale with the square root of scan rate, indicating that the redox reaction of $Ni(OH)_2$ at the graphene surface is a typical diffusion-controlled electrochemical process.[32]

3.3 Application of $Ni(OH)_2$/3DGF electrode in nonenzymatic glucose sensing

To obtain better glucose detection potential around the anodic peak on amperometric response, three different potential is investigated with successive addition of 1 mM glucose, as shown in Fig. 5a. When the detection potential is 0.5 V, an obvious current response is observed upon the each addition of glucose. At the same time, an applied potential of 0.55 and 0.6 V also can cause a notable enhancement in the current response with per addition. However, the lower potential is applied, the smaller background current and noise appears.[29] So the applied potential of 0.5 V was selected as the suitable working potential for glucose detection in the subsequent studies. Fig. 5b shows the amperometric

response of Ni(OH)$_2$/3DGF to the successive step-wise addition of glucose into a homogeneously

stirred 0.1 M NaOH solution at working potential of 0.5 V. A steep increase in current responses was

obtained after each addition of glucose solution, and a steady-state current was achieved within 5 s,

indicating the Ni(OH)$_2$/3DGF exhibits very sensitive and rapid response characteristics. This might be

due to the fact that 3DGF provides a low resistance and promotes the electron transfer to reduce the

response time.[28] The inset shows the current response of the electrode toward the addition of 1 and 2

μM glucose. The corresponding calibration curve presented in Fig. 5c is liner over a concentration

range from 1 μM to 1.17 mM glucose with a slop of 928.18 μA mM^{-1} and a correlation coefficient of

0.999. The sensitivity of the Ni(OH)$_2$/3DGF electrode is calculated as 2.652 mA mM^{-1} cm^{-2}. It is noted

that the current response decreases accordingly when the concentration of glucose continuously

increases to 3.57 mM, indicating all active sites of Ni-based electrode are bound to glucose substrate at

higher glucose concentration. Based on a signal-to-noise ratio of 3 (S/N=3), the detection limit can

reach 0.34 μM, suggesting the extremely high sensitivity of the electrochemical electrode. Table 1

summarizes the nonenzymatic glucose detection performance with different electrode reported

previously. It can be concluded that graphene based free-standing Ni(OH)$_2$/3DGF electrode possesses

higher sensitivity and larger liner range toward glucose detection. These superiorities are believed to be

attributed to synergistic effect of Ni(OH)$_2$ nanosheets and 3DGF, which includes the high catalytic

activity of Ni(OH)$_2$ and the electrical network formed through Ni(OH)$_2$ directly deposited on the 3D

graphene surface. Moreover, the well-distributed Ni(OH)$_2$ nanosheets on the surface of graphene can

favor single Ni(OH)$_2$ nanoparticles easily accessing to glucose, which significantly enhance the

electrochemical response toward glucose oxidation.

Beside sensitivity, selectivity is another major factor to assess the performance of the Ni(OH)$_2$/3DGF

electrode for nonenzymatic glucose detection. Except glucose, the effects of five other kinds of interferential compounds, including DA, lactose, D-fructose, AA and urea on the electrochemical response are investigated. Considering the concentration of glucose is more than 30 times of interfering species in human serum, the interference experiment was performed by successive addition of 1 and 0.5 mM glucose and 0.1 mM other interferences in 0.1 M NaOH. As shown in Fig 5d, both remarkable current enhancements are observed by the addition of 1 and 0.5 mM glucose. On the contrary, there are no evident current response with the addition of interfering species compared with adding glucose. These results indicated that the $Ni(OH)_2$/3DGF could be used for the sensitive and selective detection of glucose with negligible interference from DA, lactose, D-fructose, AA and urea.

4. Conclusion

In conclusion, a novel composite with hexagonal $Ni(OH)_2$ nanosheets deposited on the surface of 3D graphene foam is synthesized through a facial hydrothermal process without any auxiliary reagents. Serving as a free-standing electrochemical electrode, the $Ni(OH)_2$/3DGF presents excellent nonenzymatic glucose sensing performance in terms of sensitivity, selectivity, response time and linear calibration. The greatly enhanced electrochemical catalytic reactivity can be attributed to high electrocatalytic activity provided by $Ni(OH)_2$ nanosheets and high electrochemical active surface area from graphene foam. Moreover, the experiment extends the 2D graphene into 3D architecture and functional hybrids successfully. It will be the most promising composites for fabricating 3DGF supported metal oxide nanostructures for practical nonenzymatic glucose sensors.

References

1   M. S. Steiner, A. Duerkop and O. S. Wolfbeis, *Chem. Soc. Rev.*, 2011, **40**, 4805.

2   K. Länge, B. E. Rapp and M. Rapp, *Anal. Bioanal. Chem.*, 2008, **391**, 1509.

3   P. R. Miller, S. A. Skoog, T. L.Edwards, D. R. Wheeler, X. Xiao, S. M. Brozik, R. Polsky and R. J. Narayan, *Journal of visualized experiments: JoVE.*, 2012, **64**, e40676.

4   K. Billingsley, M. K. Balaconis, J. M. Dubach, N.Zhang, E. Lim, K. P. Francisand and H. A. Clark, *Anal. Chem.*, 2010, **82**, 3707.

5   Y. X. Huang, X. C. Dong, Y. M. Shi, C. M. Li, L. J. Li and P. Chen, *Nanoscale*, 2010, **2**, 1485.

6   J. Wang, *Chem. Rev.*, 2008, **108**, 814.

7   Z. G. Zhu, L. Garcia-Gancedo, A. J. Flewitt , H. Q. Xie , F. Moussy and W. I. Milne, *Sensors*, 2012, **12**, 5996.

8   N. Q. Dung, D. Patil, H. Jung and D. Kim, *Biosens. Bioelectro.*, 2013, **42**, 280.

9   F. Xiao, Y. Q. Li, H. C. Gao, S. B. Ge and H. W. Duan, *Biosens. Bioelectro.*, 2013, **41**, 417.

10   P. Subramanian J. Niedziółka-Jönsson, A. Lesniewski, Q. Wang, M. Li, R. Boukherroub and S. Szunerits, *J. Mater. Chem. B*, 2014, **2**, 5525.

11   C. Y. Ko, J. H. Huang, S. Raina and W. P. Kang, *Analyst*, 2013, **138**, 3201.

12   J. T. Li, W. Zhao, F. Q Huang, A. Manivannan and N. Q. Wu, *Nanoscale*, 2011, **3**, 5103.

13   H. L. Li, S. Q. Liu, C. H. Huang, Z. Zhou, Y. H. Li and D. Fang, *Electrochimica Acta*, 2011, **58**,

89.

14   Y. X. Liu, X. C. Dong and P. Chen, *Chem. Soc. Rev.*, 2012, **41**, 2283.

15   A. Kasry, M. A. Kuroda, G. J. Martyna, G. S. Tulevski and A. A. Bol, *ACS Nano*, 2010, **4**, 3839.

16   X. C. Dong, J. X. Wang, J. Wang, M. B. Chan-Park, X. A. Li, L. H. Wang, W. Huang and P. Chen, *Mater. Chem. Phys.*, 2012, **134**, 576.

17   X. C. Dong, Y. M. Shi, W. Huang, P. Chen and L. J. Li, *Adv. Mater.*, 2010, **22**, 1649.

18   T. Maiyalagan, X. C. Dong, P. Chen and X. Wang, *J. Mater. Chem.*, 2012, **22**, 5286.

19   Z. P. Chen, W. C. Ren, L. B. Gao, B. L. Liu, S. F. Pei and H. M. Cheng, *Nat. Mater.*, 2011, **10**, 424.

20   X. C. Dong, Y. F. Cao, J. Wang, M. B. Chan-Park, L. H. Wang, W. Huang and P. Chen, *RSC Adv.*, 2012, **2**, 4364.

21   Y. H. Chang, C. T. Lin, T. Y. Chen, C. L. Hsu, Y. H. Lee, W. Zhang and L. J. Li, *Adv. Mater.*, 2013, **25**, 756.

22   X. C. Dong, X. W. Wang, L. H. Wang, H. Song, H. Zhang, W. Huang and P. Chen, *ACS Appl. Mater. Interfaces* 2012, **4**, 3129.

23   A. Reina, X. T. Jia, J. Ho, D. Nezich, H. B. Son, V. Bulovic, M. S. Dresselhaus and J. Kong, *Nano Lett.,* 2009, **9**, 30.

24   W. J. Zhou, X. H. Cao, Z. Y. Zeng, W. H. Shi, Y. Y. Zhu, Q. Y. Yan, H. Liu,J. Y. Wang and H. Zhang, *Energy. Environ. Sci.*, 2013, **6**, 2216.

25   N. Q. Qiao and J. B. Zheng, *Microchim Acta*, 2012, **177**,103.

26   Y. M. Jiang, S. J. Yu, J. J. Li, L. P. Jia and C. M. Wang, *Carbon*, 2013, **63**, 367.

27   L. Zheng, J. Q. Zhang, J. F. Song, *Electrochim. Acta*, 2009, **54**, 4559.

28   H.G. Nie, Z. Yao, X. M. Zhou, Z. Yang, S. M. Huang, *Biosens. Bioelectro.*, 2011, **30**, 28.

29   Y. Zhang, F. G. Xu, Y. J. Sun, Y. Shi, Z. W. Wen, and Z. Li, J. Mater. Chem., 2011, **21**, 16949.

30   Y. Liu, H. Teng, H.Q. Hou and T.Y. You, *Biosens. Bioelectron.*, 2009, **24**, 3329.

31   X. H. Niu, M. B. Lan, H. L. Zhao and C. Chen, *Anal. Chem.*, 2013, **85**, 3561.

32   M. Tyagi, M. Tomar and V. Gupta, *Biosens. Bioelectro.*, 2014, **52**, 196.

33   S. Q. Ci, T. Z. Huang, Z. H. Wen, S. M. Cui, S. Mao, D. A. Steeber and J. H. Chen, *Biosens. Bioelectro.*, 2014, **54**, 251.

34   X. C. Dong, H. Xu, X. W. Wang, Y. X. Huang, M. B. Chan-Park, H. Zhang, L. H. Wang, W. Huang and P. Chen, *ACS nano.* 2012, **6**, 3206.

35   P. Si, X. C. Dong, P. Chen and D. H. Kim, *J. Mater. Chem. B*, 2013, **1**,110.

36   Y. Ding, Y. Wang, L. A. Su, M. Bellagamba, H. Zhang and Y. Lei, *Biosens. Bioelectron.*, 2010, **26**, 542.
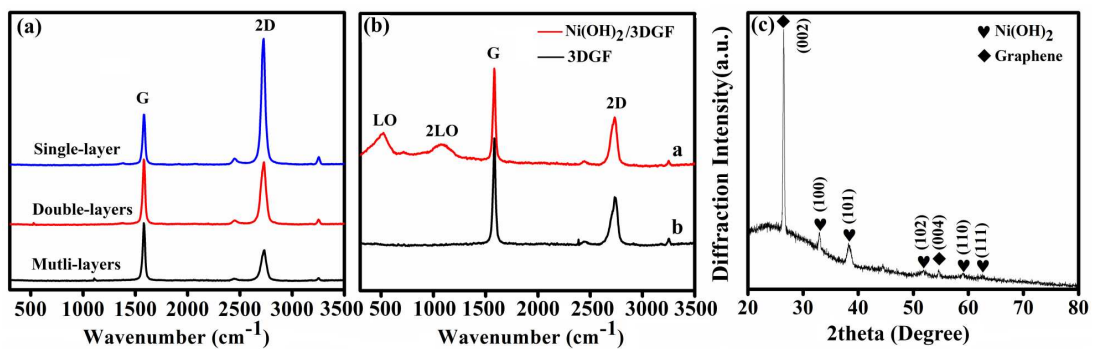
Fig. 1 (a, b) Raman spectrum of bare 3D graphene and Ni(OH)$_2$/3DGF. (c) XRD pattern of

Ni(OH)$_2$/3DGF.
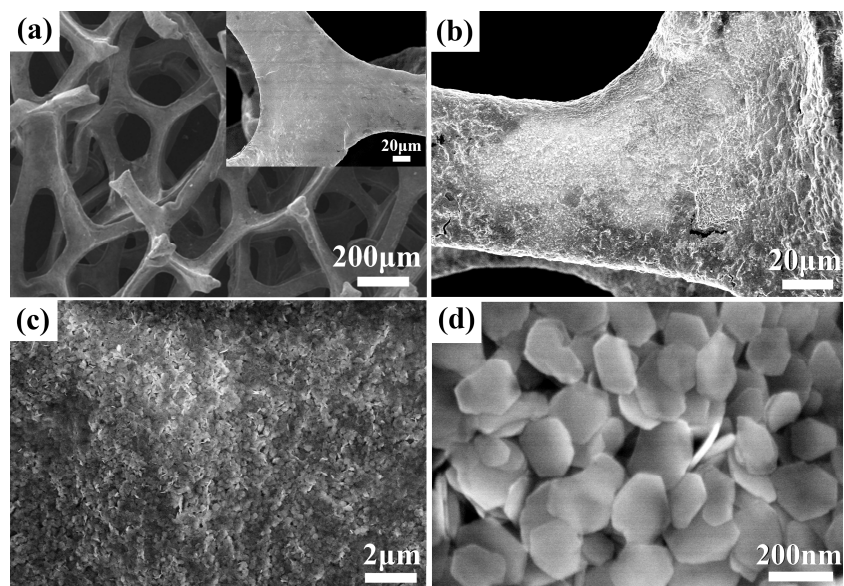
Fig. 2 (a) SEM image of bare 3D graphene foam. The inset shows the high-magnification SEM image.

(b, c) Low- and (d) high-magnification SEM images of Ni(OH)$_2$/3DGF.
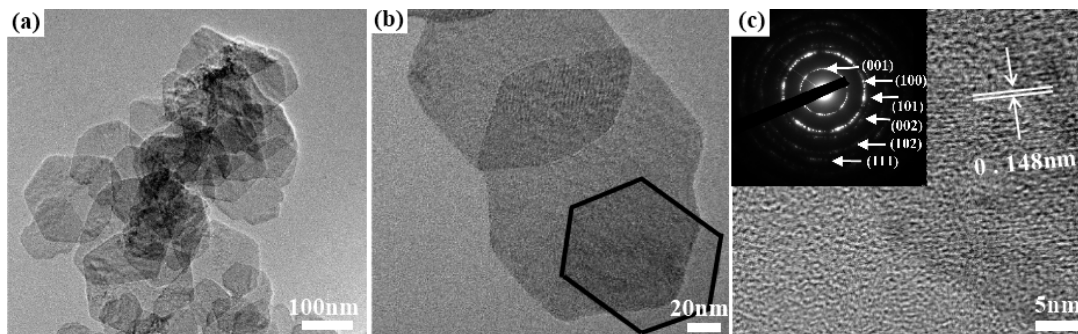
Fig. 3 (a, b) Low- and (c) high-resolution TEM images and SAED pattern (inset) of Ni(OH)$_2$ nanosheets.
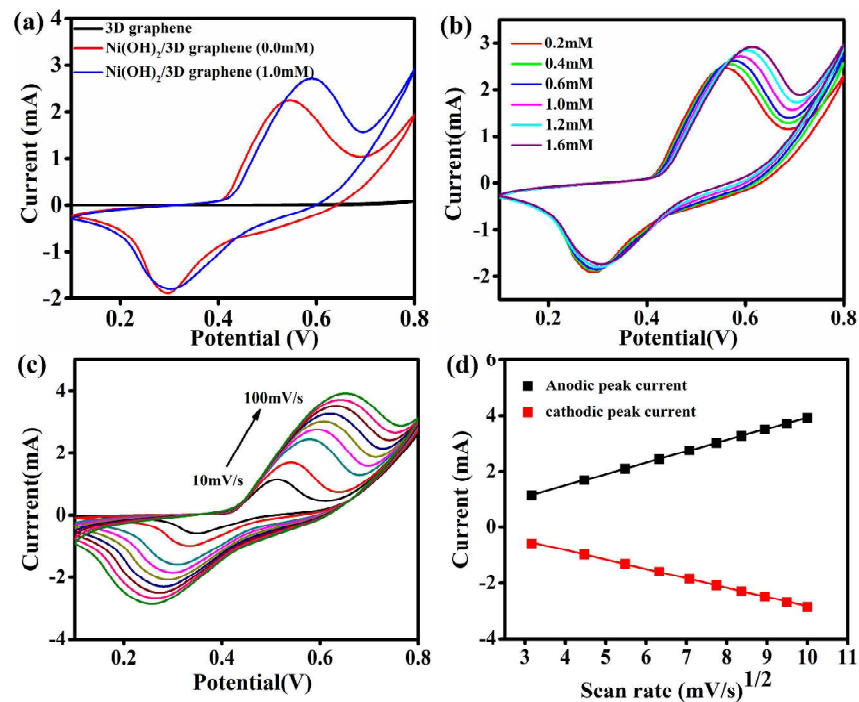
Fig. 4 (a) CVs of bare 3DGF and Ni(OH)$_2$/3DGF electrode in 0.1 M NaOH with and without 1 mM

glucose. Scan rate 50 mV/s. (b) CVs of the Ni(OH)$_2$/3DGF electrode in 0.1 M NaOH containing

different concentrations of glucose. Scan rate 50 mV/s. (c) CVs of the Ni(OH)$_2$/3DGF electrode in 1

mM glucose at various scan rate. (d) Plots of peak currents versus the square root of scan rate.

Table 1 Comparison of the sensing properties based on the Ni(OH)$_2$/3DGF with various nonenzymatic

glucose electrode reported previously

Electrode	Sensitivity (mA mM^{-1} cm^{-2})	Detection limit (μM)	Linear range	Selectivity	Ref.
Ni(OH)$_2$/PI/CNT	2.07	0.36	1 μM - 0.8 mM	Urea, UA, AA, sucrose, lactose	26
NiO-HMSs/GCE	2.39	0.53	1.67 μM-0.42 mM	DA, AA	33
Co$_3$O$_4$/3DGF	3.39	0.025	Up to 80 μM	UA, AA, serum	34
Mn$_3$O$_4$/3DGF	0.36	10	0.1- 8 mM	AA, UA, AP, serum	35
Co$_3$O$_4$ nanofiber	0.036	0.97	Up to 2.04 mM	UA, AA	36
Ni(OH)$_2$/3DGF	2.65	0.34	1μM -1.17 mM	Urea, DA, AA, lactose, D-fructose	This work
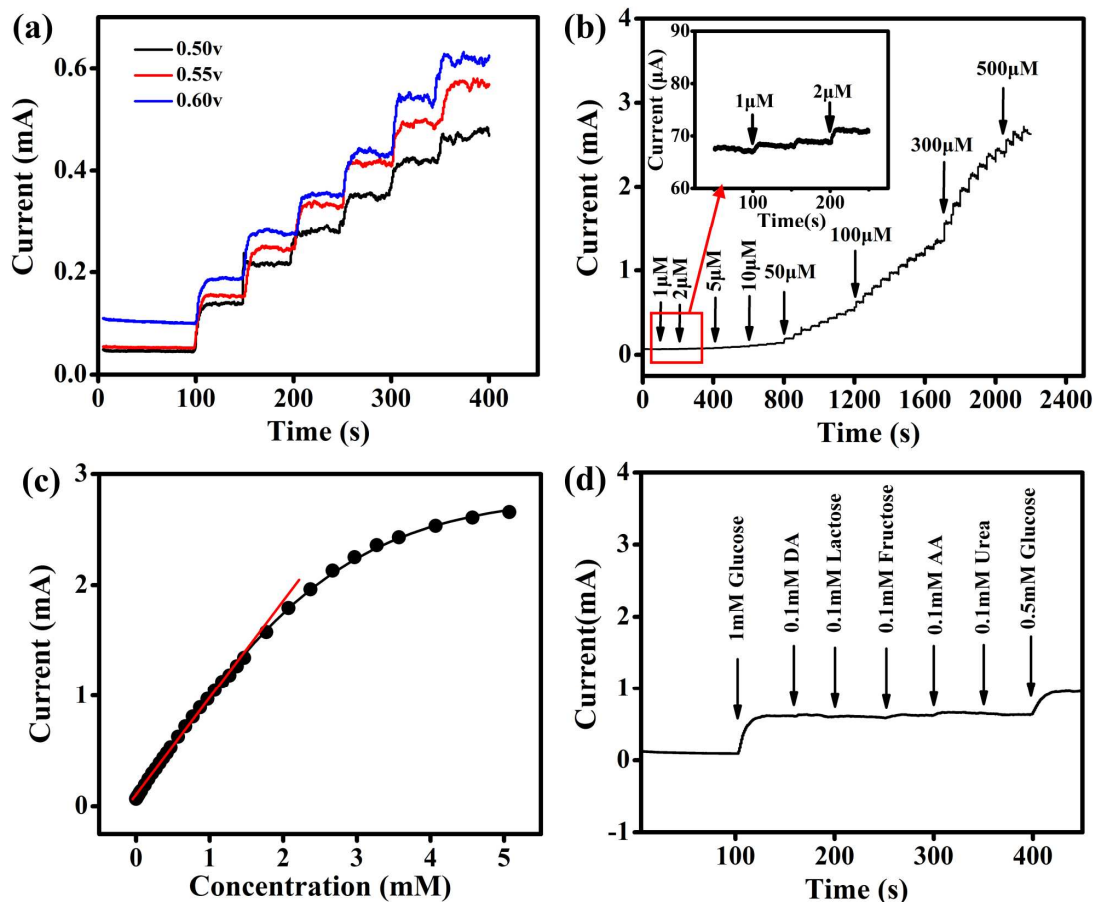
Fig. 5 (a) Amperometric response of Ni(OH)$_2$/3DGF at different potential in 0.1 M NaOH with a dropwise addition of 1 mM glucose. (b) Typical amperometric response of Ni(OH)$_2$/3DGF at 0.50 V with successive addition of glucose in 0.1 M NaOH. The inset shows the current response of the electrode toward the addition of 1 and 2 μM glucose. (c) The current response vs. glucose concentration. (d) Amperometric response of Ni(OH)$_2$/3DGF electrode toward the addition of glucose and various interferential compounds in 0.1 M NaOH.